FUSION OF OPTICAL AND INSAR FEATURES FOR BUILDING RECOGNITION IN URBAN AREAS

J. D. Wegner [a, *], A. Thiele [b], U. Soergel [a]

[a] Institute of Photogrammetry and Geoinformation, Leibniz University Hannover, Hannover, Germany –
(wegner, soergel)@ipi.uni-hannover.de

[b] FGAN-FOM Research Institute of Optronics and Pattern Recognition, Ettlingen, Germany –
thiele@fom.fgan.de

Commission III, WG III/4

KEY WORDS: Remote Sensing, Fusion, Feature Extraction, InSAR Data, Optical Data, Urban Area

ABSTRACT:

State-of-the-art space borne SAR sensors are capable of acquiring imagery with a geometric resolution of one meter while airborne SAR systems provide even finer ground sampling distance. In such data, individual objects in urban areas like bridges and buildings become visible in detail. However, the side-looking sensor principle leads to occlusion and layover effects that hamper interpretability. As a consequence, SAR data is often analysed in combination with complementary data from topographic maps or optical remote sensing images. This work focuses on the combination of features from InSAR data and optical aerial imagery for building recognition in dense urban areas. It is shown that a combined analysis of InSAR and optical data very much improves detection results compared to building recognition based on merely a single data source.

1. INTRODUCTION

Due to its independence of daylight and all-weather capability, synthetic aperture radar (SAR) has become a key remote sensing technique in the last decades. One main application scenario arises in crisis situations when the acquisition of a scene is required immediately for rapid hazard response. Urban areas play a key-role since the lives of thousands of people may be in danger in a relatively small area. In SAR data of one meter geometric resolution collected by modern space borne sensors such as TerraSAR-X and Cosmo-SkyMed, the geometric extent of individual objects like bridges, buildings and roads becomes visible. In airborne data such objects are imaged with even more detail. However, shadowing and layover effects, typical for SAR image acquisitions in urban areas, complicate interpretation. Small buildings are often occluded by higher ones while façades overlap with trees and cars on the streets. In addition, the appearance of an individual building in the image highly depends on the sensor's aspect. Buildings that are not oriented in azimuth direction with respect to the sensor are often hard to detect. This drawback can be partly overcome by using SAR images from multiple aspects (Xu and Jin, 2007). Building recognition and reconstruction can be further improved based on interferometric SAR (InSAR) acquisitions from two orthogonal flight directions (Thiele et al., 2007).

Nevertheless, automatic urban scene analysis based on SAR data alone is hard to conduct. SAR data interpretation can be supported with additional information from GIS databases or high-resolution optical imagery. Optical images have the advantage of being widely available. In (Soergel et al., 2007) high-resolution airborne InSAR data is combined with an optical aerial image in order to three-dimensionally reconstruct bridges over water. Tupin and Roux (2003) propose an approach to automatically extract footprints of large flat-roofed buildings based on line features by means of a SAR amplitude image and an optical aerial image. Furthermore, homogeneous regions in an aerial photo, represented in a region adjacency graph, are used in (Tupin and Roux, 2005) to regularize elevation data derived from radargrammetric processing of a SAR image pair by means of Markov Random Fields.

In this paper, an approach for building recognition in dense urban areas is presented that combines line features from mono-aspect InSAR data with classification results from one optical aerial image. Building corner lines extracted from InSAR data are introduced as features into a classification framework that is based on a segmentation of the optical image. Optical features and InSAR lines are jointly used in order to evaluate building hypothesis. The focus is on the fusion approach of building primitive hypothesis.

2. ANALYSIS OF OPTICAL DATA

Optical images provide high resolution multi-spectral information of urban scenes. For human interpreters they are by far more intuitive to understand than SAR data since the imaging geometry corresponds to the human eye. In aerial imagery of 0.3 meters resolution, like used in this project, building roofs become visible in great detail. In addition, façade details may appear in the image if high buildings situated far away from the nadir point of the sensor are imaged.

2.1 Appearance of Buildings

The appearance of an individual building mapped by any imaging sensor is both governed by its own properties (e.g., material, geometry) as well as by sensor characteristics (e.g., principle, spectral domain, pose), which have to be considered for recognition. For example, in optical images acquired from a near nadir perspective, building roofs are the most important features for automatic detection. Shadows are also good indicators for buildings (Fig. 1) and distinguish them, for instance, from road segments or parking lots. In western

---

* Corresponding author. This is useful to know for communication with the appropriate person in cases with more than one author.
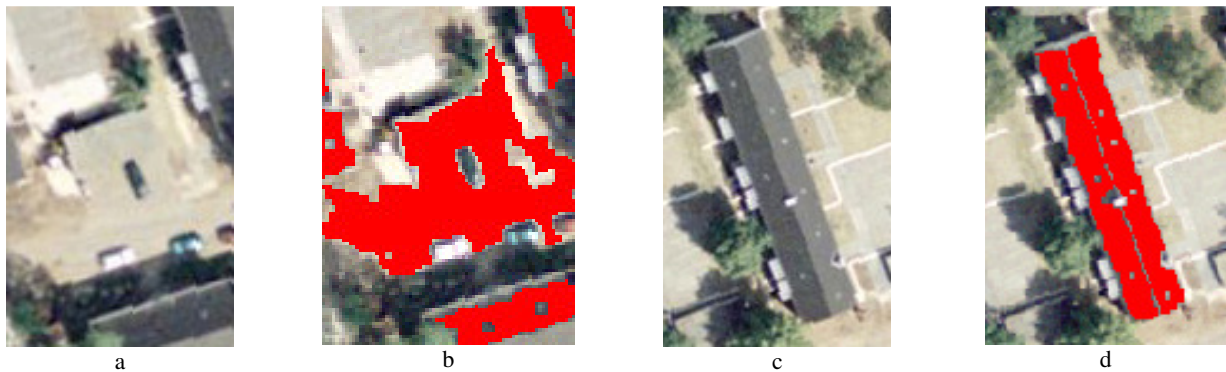
Figure 1. Flat-roofed (a) and gable-roofed (c) building in optical image overlaid with corresponding regions after segmentation (b,c)

countries rooftops look usually grey, reddish or brownish but almost never green. Roof types can roughly be subdivided into flat roofs and gable-roofs. Flat roofs coincide often with rather homogeneous image regions (Fig. 1a) while gable-roofs sometimes appear less homogeneous. Chimneys and shadows cast by chimneys may further complicate roof extraction if homogeneous planes are fit to roofs (Fig. 1 c,d). Due to similar colour of adjacent roof and street regions, such entities are sometimes hard to be told apart even for human interpreters (Fig. 1 a,b).

In this work the focus is on fusion of building primitive hypotheses delivered by approaches from the literature, tailored to the specific constraints that are determined by the particularities of the optical and microwave realm, respectively. With respect to the visible domain, a robust model-based roof detection approach introduced in Mueller and Zaum (2005), known to deliver good results, was used. It is based on an initial region growing step yielding homogeneous segments. As a consequence of the previously outlined diverse appearance of building roofs in optical imagery, such segmentation may sometimes lead to suboptimal results if contrast between roof regions and adjacent regions is very low (Fig. 1a). Thus, the region growing step can lead to erroneous roof segments (Fig. 1b). Gable-roofs usually split up into at least two segments if they are not oriented along the sun illumination direction (Fig. 1. c,d). Sometimes, gable-roofs may split up into even more than two segments and only parts are evaluated as roof regions. In such cases, the introduction of building hints from SAR data can highly improve building detection.

2.2 Feature Extraction

The building roof extraction approach consists of a low-level and a subsequent high-level image processing step (Mueller and Zaum, 2005). The low-level step includes transformation of the RGB image to HSI (Hue Saturation Intensity) representation, a segmentation of building hypotheses in the intensity image and the application of morphological operators in order to close small holes. Region growing, initialized with regularly distributed seed points on a grid, is used as image segmentation method. Seed points that fall into a grid cell which either consists of shadow or features a greenish hue value are erased and no region growing is conducted. Adjacent roof regions having a significant shadow region next to them are merged. This step is important for gable-roofed buildings because sometimes the roof is split at the roof ridge due to different illumination of the two roof parts. However, gable-roofs that were split up into more than two segments are not merged to one single segment which is the main reason for undetected buildings later-on in the process.

Features are extracted for each roof hypothesis in order to prepare for classification. Four different feature types are used, based on geometry, shape, radiometry, and structure. Geometric features are the region size and its perimeter. The shape of a building region is described by its compactness and length. Right angles, distinguishing roofs from trees in the real world, are not used as a shape feature since the region growing step may lead to segments that are not rectangular although they represent roofs (Fig. 1b). Radiometry is used in order to sort out regions with a high percentage of green pixels. Structural features are for example neighbouring building regions and shadows cast by the potential building. Shadows are good hints for elevated objects. In order to not take into account shadows cast by trees, only shadows with relatively straight borders are considered as belonging to buildings.

Finally, a classification based on the previously determined feature vector takes place (see chapter 4.2 for details). All necessary evaluation intervals and thresholds were learned from manually classified training regions.

3. ANALYSIS OF INSAR DATA

3.1 Appearance of Buildings

The appearance of buildings in InSAR data is characterized by the oblique illumination of the scene and therefore the image projection in slant range geometry. Furthermore, it depends on sensor parameters, on properties of the imaged object itself, and on the object's direct environment.

In Fig. 2 an example of flat-roofed buildings in optical (Fig. 2a) and InSAR data (Fig. 2 b,d) is given. The appearance of different building types and effects that occur if the scene is illuminated from two orthogonal flight directions have been comprehensively discussed in Thiele et al. (2007 and 2008).

The magnitude profile of a building is typically a sequence of areas of various signal properties: layover, corner reflector between ground and building wall, roof, and finally radar shadow (Fig. 2c). The layover area is the building signal situated the closest to the sensor in the image because its distance is the shortest. It usually appears bright due to superposition of backscatter from ground, façade, and roof. The layover area ends at the bright so-called corner reflector line. This salient feature is caused by double-bounce reflection at a dihedral corner reflector spanned by ground and wall along the building. This line coincides with a part of the building footprint and can be distinguished from other lines of bright scattering using the InSAR phases (see Fig. 2d and profile in Fig. 2e). The single backscatter signal of the building roof is either included in the layover mixture or scattered away from
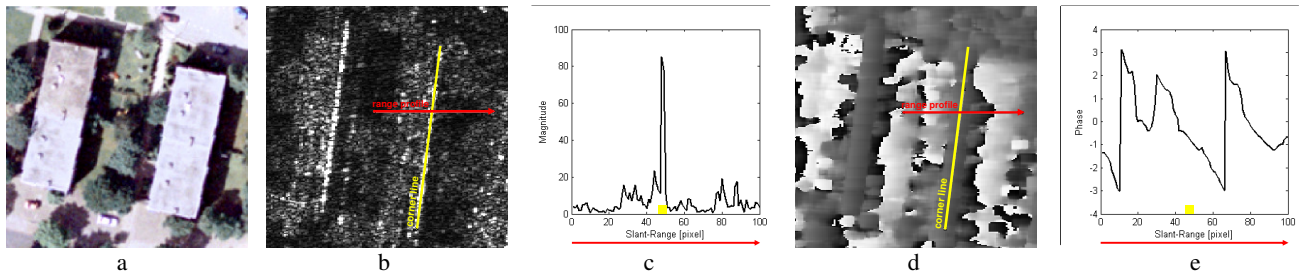
Figure 2. Appearance of flat-roofed buildings in optical data (a), in SAR magnitude data with illumination from right to left (b,c) and InSAR phase data (d,e)

the sensor depending on roof structure and illumination geometry. Ground behind the building is partly occluded by the building shadow leading to a dark region in the image.

A building also leads to specific patterns in the interferometric phase data (Fig. 2d and Fig. 2e) because the phase value of a single range cell results from a mixture of the backscatter of different contributors, such as ground, façade, and roof in the layover area. Again, the appearance is characterized by a layover region and a homogeneous roof region (in Fig. 2 not observable because of the narrow building width). The phase of the terrain enclosing the building is displayed slightly darker. A similar phase value is calculated at the building corner location, which is used for the detection of building footprints. Since no signal is received in shadow area, the related InSAR phase carries no useful signal but noise only.

3.2 Feature Extraction

This approach of building recognition in InSAR data is based on the detection of parts of the building footprint. First, the segmentation of bright lines is carried out in the magnitude data. Based on this set of lines, only the ones caused by a dihedral corner reflector spanned by ground and building wall are used as building hints. In order to exclude all lines that do not fulfil this criterion, the local InSAR heights are analysed. Finally, the filtered corner lines are projected into the same ground range geometry as the optical data.

3.2.1 Corner Line Segmentation

As previously discussed, the bright corner lines are very useful hints to buildings since they provide information about the true location of a part of the building footprint. The full process of corner line detection is shown in Fig. 3, upper row.

The line detection is carried out in slant range geometry based on the original magnitude images (Fig. 3 "Magnitude") by using an adapted ratio line detector according to Tupin et al. (1998). This template detector determines the probability of a pixel of belonging to a line. In our case, eight different template orientations are considered. The probability image for the vertical template orientation is shown in Fig. 3 "Line". Thereafter, line segments are assembled based on the eight probability images and their respective window orientation. The resulting segments are fitted to straight lines and edges, respectively, by linear approximation and subsequent prolongation (yellow lines in Fig. 3).

3.2.2 Geocoding of Building Features

After line extraction, the interferometric heights are calculated as described in (Thiele et al., 2007). Results are shown in Fig. 3 "Heights". Local InSAR heights are investigated in order to discriminate lines caused by direct reflection and lines due to double-bounce reflection between either ground and wall or roof and substructures. For this filter step, the height difference between Digital Surface Model (DSM) and Digital Terrain Model (DTM) is used.

The DSM is given by the calculated InSAR heights. In order to derive the DTM from it, a filter mask is computed to define the DSM pixels which are considered in the DTM generation. Only pixels with a high coherence value (Fig. 3 "Coherence") and an InSAR height close to the global mean terrain height are considered in equation 1 (Fig. 3 "Mask").

$$x_{mask,i} = \begin{cases} 1, if \ x_{coh,i} \geq 0.5 \ and \ \left(x_{h,i} - \overline{x_h}\right) \leq \pm\sigma_{\overline{x_h}} \\ 0, else \end{cases} \quad (1)$$

Based on this mask and the InSAR heights, a DTM height value is calculated over an area of 50 m x 50 m in ground range geometry (Fig. 3 "DTM"). Thereafter, the height differences (i.e., a normalized DSM) between DSM and DTM are calculated (Fig. 3 "Height difference").

In the following line filtering step, lines are considered as real building corner lines if their neighbouring pixels show a low mean height difference value (Fig. 3 "Height difference", rescaled for visualization). The filtered real corner lines are displayed in Fig. 3 (red lines). Final geo-coding of these corner lines is carried out using the InSAR heights. The resulting geographic position of the corner lines superimposed onto the optical image is displayed for the entire test site in Fig. 5b.

4. FUSION OF EXTRACTION OUTCOMES

In order to accurately combine features from InSAR data and the optical image, different sensor geometries and projections have to be considered carefully. It is required that both feature sets are projected to the same geometry, i.e., all data have to be transformed to a common coordinate system (Thiele et al., 2006). In addition, a fusion and classification framework for combining the detection outcomes from the optical image and from the InSAR data has to be set up.

| Magnitude | Line | Coherence | Height difference with segmented lines | Magnitude with detected building corners |

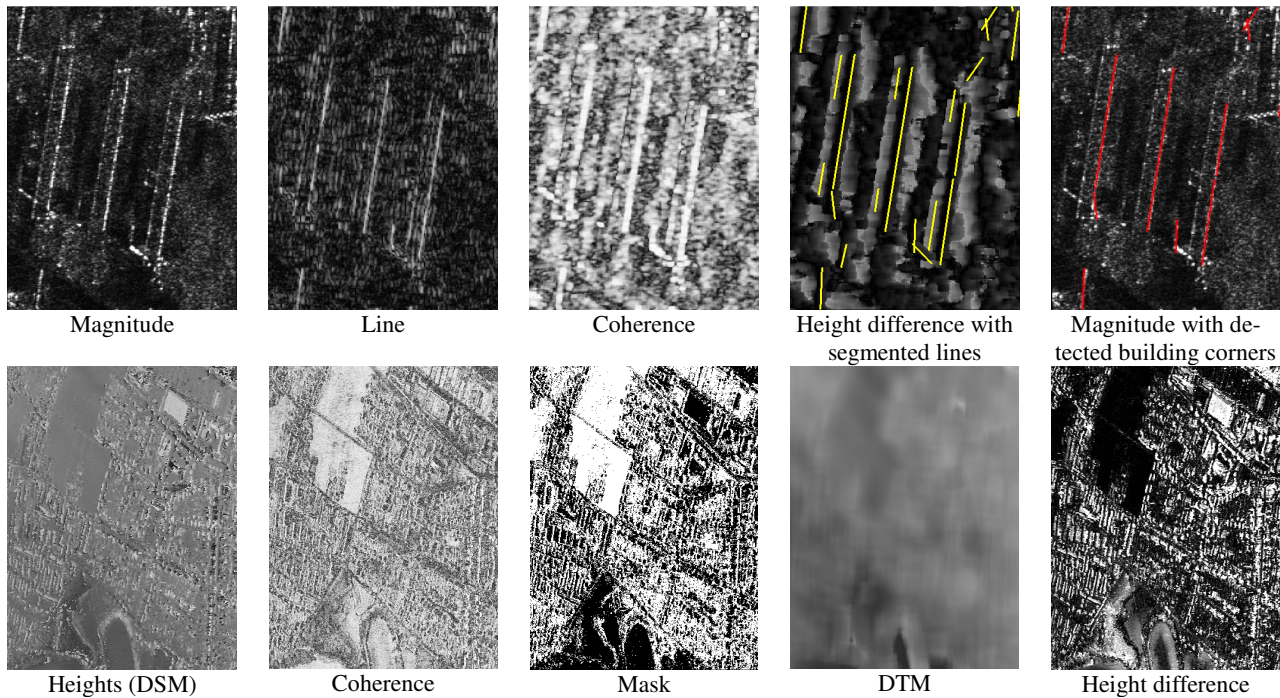| Heights (DSM) | Coherence | Mask | DTM | Height difference |

Figure 3. Upper row: steps of building corner segmentation in slant range geometry with illumination direction from left to right; lower row: steps of the InSAR height filtering and slant range to ground range projection of the building corner lines

4.1 Sensor geometries

The particularities of Synthetic Aperture Radar (SAR) and optical cameras in terms of sensor principle and viewing geometry result in very different properties of the observed objects in the acquired imagery. In Fig. 4a an elevated object P of height h above ground is imaged by both a SAR sensor and an optical sensor (OPT). SAR is an active technique measuring slant ranges to ground objects with a rather poor angular resolution in elevation direction. Layover, foreshortening, and shadowing effects consequently occur and complicate the interpretation of urban scenes. Buildings therefore are displaced towards the sensor. Point P in Fig. 4a is thus mapped to point PS in the image. The degree of displacement depends on the object height h and the off-nadir angle θ_1 of the SAR-sensor.

By contrast, optical sensors are passive sensors acquiring images with small off-nadir angles. No distances but angles to ground objects are measured. Elevated objects like P in Fig. 4a that are not located directly in nadir view of the sensor are displaced away from the sensor. Instead of being mapped to P', P is mapped to PO in the image. The degree of displacement depends on the distance between a building and the sensor's nadir point as well as on a building's height. The further away an elevated object P is located from the nadir axis of the optical sensor (increasing θ_2) and the higher it is, the more the building roof is displaced. The higher P is, the further away P is located from the optical nadir axis and the greater the off-nadir angle θ_1 becomes, the longer the distance between PO and PS will get.

The optical data was ortho-rectified by means of a DTM in order to reduce image distortions due to terrain undulations. Building façades stay visible and roofs are displaced away from the sensor nadir point since buildings are not included in the DTM. Such displacement effect can be seen in Fig. 4b to 4d. In Fig. 4b the building in the optical image is overlaid with its cadastral boundaries. The building roof is displaced to the right since the sensor nadir point is located on the left. The upper right part of the building is more shifted to the right than the

lower left part because it is higher (see Fig. 4d for building height). Fig. 4c shows the same cut-out overlaid with the corner line extracted from the corresponding InSAR cut-out. Such corner line represents the location where the building wall meets the ground which can nicely be seen in Fig. 4d. Due to the previously outlined perspective effect the building roof falls to the right over the corner line. This effect is of high interest and can be exploited for three-dimensional modelling of the scene (Inglada and Giros, 2004, Wegner and Soergel, 2008) because the distance between the corner line and the building edge comprises height information.

4.2 Joint classification framework

A joint classification is carried out after having projected the optical and the InSAR primitive objects to the same ground geometry. In order to combine the building hints from optical and InSAR data, a fusion step is required. One possibility is data fusion in a Bayesian framework while another would be Dempster-Shafer evidential theory (Klein, 2004). Both approaches are usually requiring an object to be represented identically in the different sensor outputs, i.e., exactly the same region is found in both datasets but with slightly different classification results. This requirement is not met in the case of the combination of line features from InSAR data with roof regions from optical imagery.

Hence, combined analysis is based on the linear regression classifier already used for building extraction from optical data in (Mueller and Zaum, 2005). All potential building objects from the optical image are evaluated based on a set of optical features described in section 2.2 and on the InSAR corner line objects. The evaluation process is split up into two parts, an optical part and an InSAR part. Optical primitive objects are believed to contribute more information to building detection and hence their weight is set to two thirds. InSAR data is assumed to contribute less information to overall building recognition and thus the weight of primitive objects derived
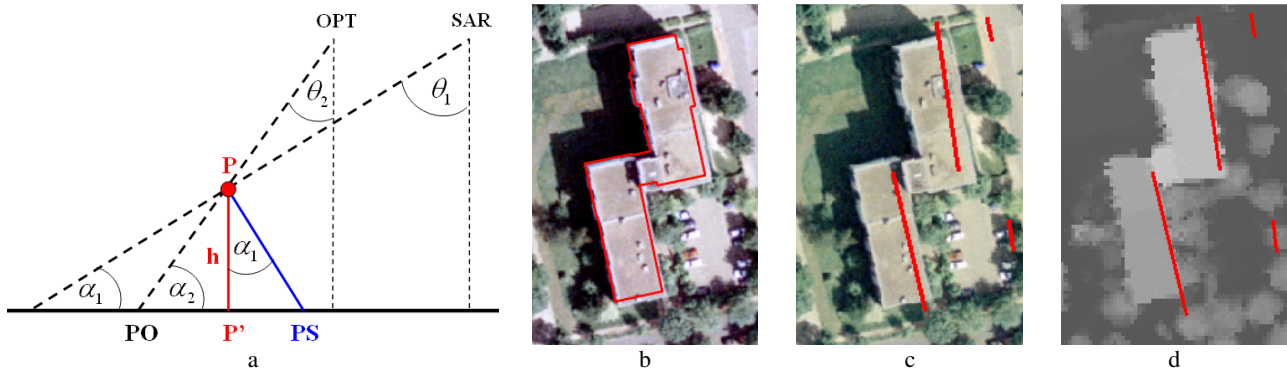
Figure 4. Comparison of SAR and optical viewing geometry under the assumption of locally flat terrain (a); optical data (b) overlaid with cadastral building footprint; optical data (e) and LIDAR data (d) overlaid with detected building corner

from SAR data is set to one third. Such weights are determined empirically and lead to good results. However, further research has to be done in order to support this choice with reasonable statistics.

A quality measure is assigned to each region and initially set to 1. In the first evaluation part each primitive is evaluated based on the optical feature vector. Each time a feature does not completely support the building hypothesis, the quality measure is reduced by multiplication with a value between 0 and 1. The exact reduction value for each feature was learned on manually labelled training data. Such reduced quality measure is again multiplied with another reduction value if another feature partly rejects a building hypothesis. The final quality measure based on the optical feature vector is weighted with 0.666.

A second region evaluation is conducted based on the corner line primitives extracted from InSAR data. First, all building object hypotheses are enlarged by two subsequent dilation operations. In this manner, a two-pixel wide buffer, corresponding to 0.6 meters in ground geometry, is added to the original region since building roofs may be shifted away from the corner line. Thereafter, it is checked if the corner line crosses this enlarged region with a certain minimum length. The initial quality measure is multiplied with a reduction value like in the optical case if this is not the case. The resulting quality measure based on the corner line is multiplied with a weighting factor of 0.333.

Finally, the overall quality measure is obtained by summing up the optical and the InSAR quality measures. In case neither an optical feature nor an InSAR feature has decreased the quality measure, both quality measures sum up to one. All regions that have a quality measure greater than an empirically determined threshold are classified as building objects. Such threshold was set to 0.6. As a consequence, a region may be classified as building region even if there is no hint from the InSAR data, but strong evidence from the photo. The reason is that some buildings do not show corner lines due to an unfavourable orientation towards the SAR-sensor (see the gabled-roofed buildings in the lower right corner of Fig. 5b) or occlusion of the potential corner line region by plants. On the contrary, a region cannot be evaluated as building region based merely on the corner line which are strong hints for buildings but may also caused by other abrupt height changes in urban areas.

5. RESULTS

The InSAR data used in this project was recorded by the AeS-1 sensor of Intermap Technologies. The spatial resolution in range is about 38 cm while 16 cm resolution is achieved in azimuth direction. The two X-Band sensors were operated with

an effective baseline of approximately 2.4 m. The mapped residential area in the city of Dorsten in Germany is characterized by a mixture of flat-roofed and gable-roofed buildings and low terrain undulation.

Results of the presented approach for building recognition by means of feature combination from optical imagery and InSAR data are shown in Fig. 5. In Fig. 5a building recognition results based solely on optical features are displayed. All parameters where specifically adjusted in order to achieve the lowest possible false alarm rate while still detecting buildings. Less than 50% of the buildings contained in the displayed scene are detected. In addition, false alarms could not be avoided completely. Results are rather poor due to the assumption that roofs do not split up into more than two regions during the region growing step, which is not met for the data at hand. As a consequence, several gable-roofed buildings with reddish roofs in the lower right corner of the image could not be recognized. Some big flat-roofed buildings in the upper part of the image are not detected because their colour and shape are similar to such of street segments. Thus, their evaluation value does not exceed the threshold.

Fig. 5b shows the corner lines extracted from the InSAR data superimposed onto one SAR magnitude image. An InSAR corner line could be detected for almost all buildings in this scene. Some lines are split into two parts because the corresponding building was partly occluded by, e.g., plants. Some corner lines in the lower right diagonally cross buildings which is not plausible. Most likely this effect is an artefact introduced by too large tolerances applied in the merging and prolongation steps of adjacent line segments. The final building recognition result using both optical and InSAR features is shown in Fig. 5c. The overall building recognition rate could be significantly improved to approximately 80% by integration of the InSAR corner lines into the classification procedure. Additionally, all false alarms could be suppressed. However, the gable-roofed buildings in the lower right corner stay undetected although InSAR corner lines are present. Such missed detections are due to the over-segmentation of the rather inhomogeneous roof regions in the optical image.

6. CONCLUSION AND OUTLOOK

In this work, first building detection results from combined optical and InSAR data on feature level were presented. A rather simple approach for feature fusion was introduced leading to a significantly improved building recognition rate. Additionally, the number of false alarms could be reduced considerably by the joint use of optical and InSAR features. Corner lines from InSAR data proved to be essential hints for
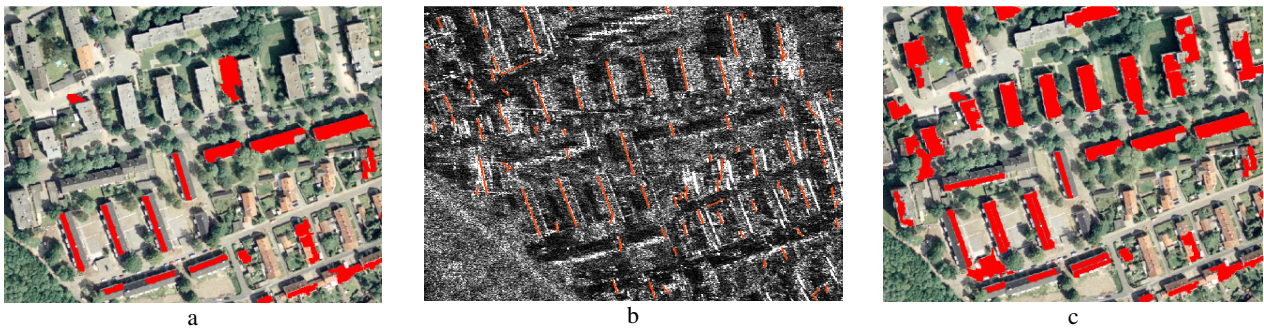
Figure 5. Results of building detection based on optical data (a), detected corner lines in the InSAR data (b), and of building detection based on InSAR and optical data (c)

buildings. Such corner lines also appear in single SAR images and hence this approach is not limited to InSAR data.

Further developed, this approach may be the basis for a change detection method after natural hazards like flooding and hurricanes. An optical image acquired before the hazard and SAR data acquired afterwards can be analyzed using the presented approach. A human interpreter would only have to check those buildings for damages that were not detected from both data sources. Hence, all buildings recognized from the combination of optical and SAR features, shown in red in Fig. 5c, would be classified as undamaged. Only buildings in the optical image that where not detected would have to be checked speeding up the entire damage assessment step significantly.

Although first results are encouraging, further improvements have to be made. One main disadvantage of the presented classification approach is that its quality measures are not interpretable as probabilities in a Bayesian sense. Although many parameters have been learned from training data, parts of the approach are still ad-hoc. A next step will thus be the integration of the presented approach into a Bayesian framework.

Furthermore, the differences of the sensor geometries should be used for further building recognition enhancement. Since the roofs of high buildings are displaced away from the sensor and parts of the façade appear in the image, roof regions have to be shifted towards the sensor in order to delineate building footprints. Such displacement also bears height information which may be used as an additional feature for building recognition. More height information may also be derived directly from the InSAR data.

Finally, three-dimensional modelling of the scene could be accomplished based on the building footprints, a height hypothesis and maybe even the estimation of the roof type. An iterative joint classification and three-dimensional modelling in a Bayesian framework, including context information, will be the final goal of this project.

7. REFERENCES

Inglada, J., and Giros, A. 2004. On the possibility of Automatic Multisensor Image Registration. IEEE Transactions on Geoscience and Remote Sensing, Vol. 42, No. 10, pp. 2104-2120.

Klein, L. A. 2004. Sensor and Data Fusion-A Tool for Information Assessment and Decision Making, 3rd ed., Bellingham, WA: SPIE Press, pp.127-181.

Mueller, S., and Zaum, D. W. 2005. Robust Building Detection in Aerial Images. IntArchPhRS, Vol. XXXVI, Part B2/W24, pp. 143-148.

Soergel, U., Thiele, A., Cadario, E., Thoennessen, U. 2007. Fusion of High-Resolution InSAR Data and optical Imagery in Scenes with Bridges over water for 3D Visualization and Interpretation. In: *Proceedings of Urban Remote Sensing Joint Event 2007 (URBAN2007)*, 6 pages.

Thiele, A., Schulz, K., Thoennessen, U., Cadario, E. 2006. Orthorectification as Preliminary Step for the Fusion of Data from Active and Passive Sensor Systems. In: *Proceedings of the IEEE International Conference on Multisensor Fusion and Integration for Intelligent Systems 2006 (MFI2006)*, 6 pages.

Thiele, A., Cadario, E., Schulz, K., Thoennessen, U., Soergel, U. 2007. Building Recognition From Multi-Aspect High-resolution InSAR Data in Urban Areas. IEEE Transactions on Geoscience and Remote Sensing, Vol. 45, No. 11, pp. 3583-3593.

Thiele, A., Cadario, E., Schulz, K., Thoennessen, U., Soergel, U. 2008. Reconstruction of residential buildings from multi-aspect InSAR data. In: *Proceedings of ESA-EUSC Workshop*, Frascati, Italy, available http://earth.esa.int/rtd/Events/ESA-EUSC_2008/, 6p.

Tupin, F., Maitre, H., Mangin, J.-F., Nicolas, J-M., Pechersky, E. 1998. Detection of Linear Features in SAR Images: Application to Road Network Extraction. IEEE Transactions on Geoscience and Remote Sensing, Vol. 36, No. 2, pp. 434-453.

Tupin, F., and Roux, M. 2003. Detection of building outlines based on the fusion of SAR and optical features. ISPRS Journal of Photogrammetry and Remote Sensing, Vol. 58, pp. 71-82.

Tupin, F., and Roux, M. 2005. Markov Random Field on Region Adjacency Graph for the Fusion of SAR and Opitcal Data in Radargrammetric Applications. IEEE Transactions on Geoscience and Remote Sensing, Vol. 42, No. 8, pp. 1920-1928.

Wegner J.D., and Soergel, U. 2008. Bridge height estimation from combined high-resolution optical and SAR imagery. IntArchPhRS, Vol. XXXVII, Part B7-3, pp. 1071-1076.

Xu, F., Jin, Y.-Q. 2007. Automatic Reconstruction of Building Objects From Multiaspect Meter-Resolution SAR Images. IEEE Transactions on Geoscience and Remote Sensing, Vol. 45, No. 7, pp. 2336-2353.